

Free electricity tandem-twin-hybrid solar-biomass dryer increased the performance of coffee cherry drying

YUWANA YUWANA*, SYAFNIL SYAFNIL

Department of Agricultural Technology, Faculty of Agriculture, University of Bengkulu, Bengkulu, Indonesia

*Corresponding author: yuwana@unib.ac.id

Citation: Yuwana Y., Syafnil S. (2025): Free electricity tandem-twin-hybrid solar-biomass dryer increased the performance of coffee cherry drying. *Res. Agr. Eng.*, 71: 174–187.

Abstract: A free electricity tandem-twin-hybrid-solar-biomass dryer comprised of two drying rooms and operated with solar and biomass energy combustion of 10 kg rubber wood per hour separately to dry Robusta coffee cherries with 3, 6, 9, and 12 cm bed thicknesses were studied with the drying completion time (tc), number of defects (ND), and colour parameters, i.e., lightness (L^*), hue angle [$H(^{\circ})$], and chroma (C), used as the performance indicators. The experimental results indicated that the drying room, bed thickness, and drying room-bed thickness interaction significantly affected the tc and ND and bed thickness only significantly affected C for both the solar energy drying and the biomass energy drying. The solar energy drying generated a drying air temperature of 44.6 ± 3.5 °C with a tc of 70.9–90.2 h for the front drying room and 40.1 ± 2.8 °C with a tc of 77.2–116.5 h for the rear drying room, whereas the biomass energy drying produced a drying air temperature of 57.2 ± 3.6 °C with a tc of 34.1–44.9 h for the front drying room and 45.6 ± 6.0 °C with a tc of 56.3–96.6 h for the rear drying room. Both drying processes produced coffee beans with the NDs less than 11 qualified for Grade 1 with similar colour characteristics.

Keywords: biomass energy drying; coffee bean colour; drying completion time; number of defects; solar energy drying

Drying is a determinant process in coffee bean production. This process is carried out with sun drying by most coffee growers which is constrained by many obstacles, such as bad weather conditions, labour-intensive and time-consuming processes, being prone to damage, and the loss of product leading to a reduction in their income. This fact challenges researchers to develop various

types of dryers and explore them to dry this type of product.

Coffee dryers can be classified into solar dryers, mechanical dryers, and hybrid solar dryers. Solar dryers include three categories, in which the first category consists of a drying room covered with a translucent material to transmit sunlight as well as to protect the coffee being dried

Financially supported by the University of Bengkulu (Agreement Contract No. 2973/UN30.15/PT/2024).

© The authors. This work is licensed under a Creative Commons Attribution-NonCommercial 4.0 International (CC BY-NC 4.0).

(Firdissa et al. 2022; Peñuela-Martínez et al. 2023), called the direct type. The second category of solar dryer is made of a drying room covered with an opaque material and equipped with a solar heat collector as a heat supplier for the coffee drying inside it (Gachen et al. 2020; Hudin et al. 2021; Oria and Palconit 2022; Mackpayen et al. 2023), called the indirect type. The third category is called a mixed type, which is a combination of the first and second categories where the dryer receives the heat directly from the sunlight passing through the walls and/or roof of its drying room and the heat supply comes from the solar heat collector (Siagian et al. 2024). In terms of the drying air circulation, many solar dyers use natural convection flow (Hudin et al. 2021; Firdissa et al. 2022) and many others use forced flow by employing a fan/blower (Oria and Palconit 2022; Mackpayen et al. 2023; Peñuela-Martínez et al. 2023). Solar dryers have been widely explored to operate with an air temperature range of 31 °C to 70 °C (Oria and Palconit 2022; Mackpayen et al. 2023) and an air-flow velocity of 0.1 ms⁻¹ to 1.5 ms⁻¹ (Hudin et al. 2021; Mackpayen et al. 2023) with a capacity of 29 kg (Putra and Hadi 2013) to 38.8 tonnes (Widyotomo 2014).

Mechanical dryers are characterised by four main components, i.e., a drying chamber to place the coffee being dried, a heater for hot air production, a duct to channel the hot air, and a fan/blower to deliver the hot air from the heater through the duct into the drying room to circulate the hot air around the coffee to evaporate its moisture content then to exhaust the moist air from the drying room (Murdianto and Santoso 2019; Phitakwinai et al. 2019; Prasetya et al. 2020; Konsil et al. 2023). There are several types of mechanical dryers such as cabinet dryers (Nasrin et al. 2021; Largo-Avila et al. 2023), rotary dryers (Prasetya et al. 2020), batch dryers (Murdianto and Santoso 2019), thin layer dryers (Phitakwinai et al. 2019; Firdissa et al. 2022) and fluidised dryer (Sutrisno et al. 2020; Konsil et al. 2023; Soeswanto et al. 2023). The dryers employ various heat sources, from electricity (Phitakwinai et al. 2019; Nasrin et al. 2021; Firdissa et al. 2022; Soeswanto et al. 2023), to liquefied petroleum gas (LPG) (Murdianto and Santoso 2019; Prasetya et al. 2020; Sutrisno et al. 2020), to moist air from drying chambers (Dzaky et al. 2023), and to exhaust gas from biomass-fuelled power plants (Al-Kindi et al. 2015) to produce a drying

air temperature of 27.3 °C to 120 °C (Nasrin et al. 2021; Konsil et al. 2023) with a drying air velocity of 2 ms⁻¹ to 10 ms⁻¹ (Sutrisno et al. 2020; Konsil et al. 2023) and dryer capacities from 1 kg (Sutrisno et al. 2020) to 20 tonnes (Hidayat et al. 2018).

Hybrid solar dryers work by utilising solar energy, both direct and/or indirect, and other sources of energy substitutes, such as electricity (Nasrin et al. 2021), LPG (Suherman et al. 2020), biomass (Irwansyah et al. 2019; Fatharani et al. 2023; Yuwana and Sidebang 2023), and geothermal heat (Gunawan et al. 2021) that can be supplied separately or simultaneously. The main structure of these dryers usually consists of a drying room, a solar collector, and a heat-generating unit or stove to provide the heat substitution. The reported hybrid solar dryers operate with a temperature range of 37.3 °C to 60.9 °C (Irwansyah et al. 2019; Chan et al. 2020) and a drying air velocity of 0.22 ms⁻¹ to 4.5 ms⁻¹ (Yani and Fajrin 2013; Irwansyah et al. 2019) with a loading capacity of 5 kg (Irwansyah et al. 2019) to 800 kg of coffee beans or cherries (Chan et al. 2020).

Currently, there are two main discrepancies of hybrid solar dryers, the first is their dependence on electricity, which increases the operating costs and is not adaptive to being installed in remote areas, and the second is subject to heat loss through the furnace's chimney, thereby wasting the fuel usage. To overcome this problem, a free electricity tandem-twin-hybrid solar-biomass dryer (FETTHSBD) making use of the flue gas heat of a biomass furnace has been developed. This study was conducted to investigate the performance of the FETTHSBD when operated with solar energy and biomass energy to dry Robusta coffee cherries of different bed thicknesses in the form of the drying completion time (*tc*), i.e. the time for the coffee cherry to obtain a 12% moisture content on a wet basis (w.b.), the number of defects (*ND*), and the colour of the coffee beans produced in respect to the drying rooms.

MATERIAL AND METHODS

Description and operation of the free electricity tandem twin hybrid solar-biomass dryer (FETTHSBD)

The developed FETTHSBD (Figure 1) was installed at an outdoor area of the Agricultural Technology

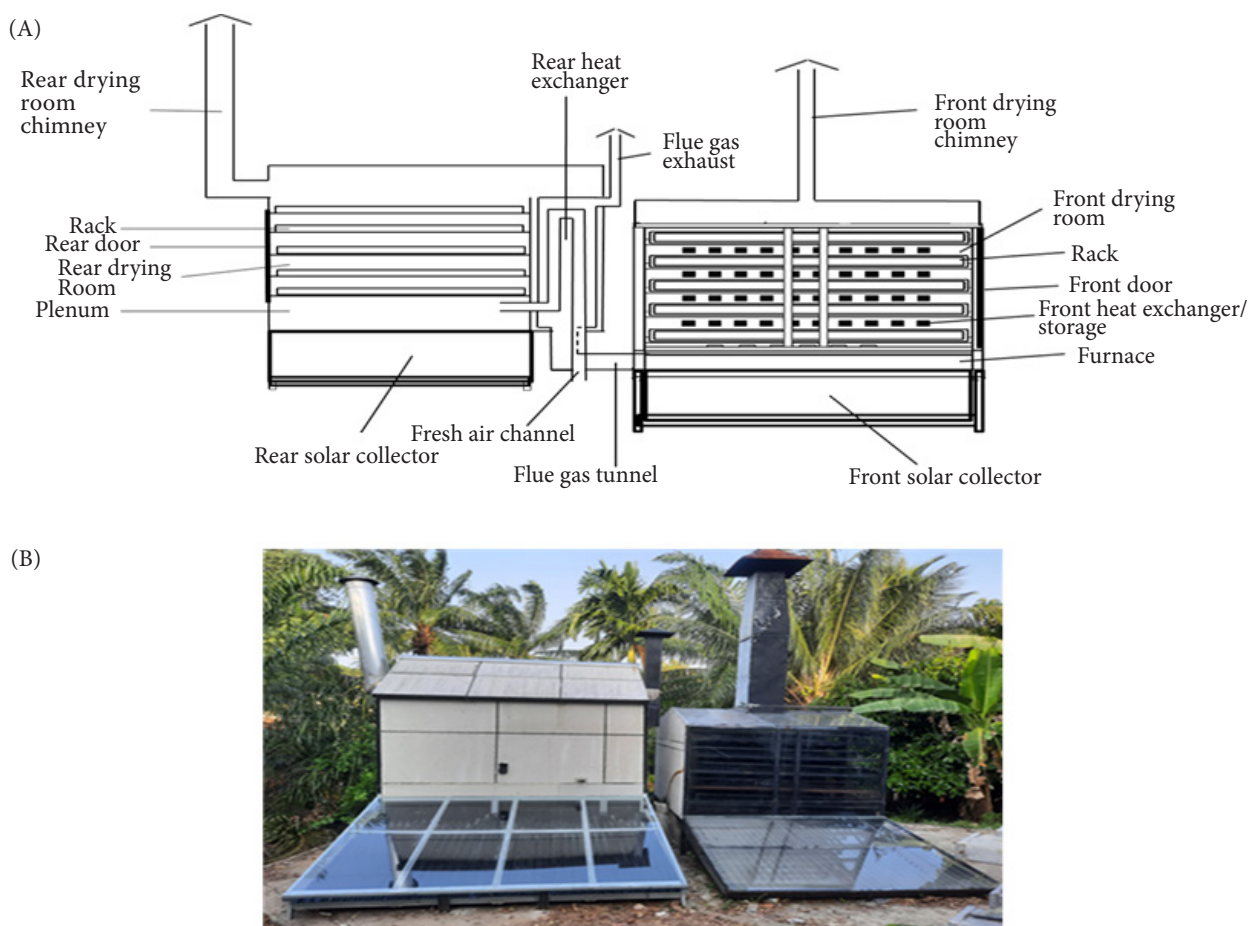


Figure 1. Free electricity twin-hybrid solar-biomass dryer – (A) design and (B) photo of the installation

Laboratory, Agricultural Technology Department, University of Bengkulu, Bengkulu City, Indonesia with a geographic location of $03^{\circ}45' - 03^{\circ}59'$ S latitude and $102^{\circ}14' - 102^{\circ}22'$ E longitude comprised of two drying rooms (front and rear), each of them equipped with two solar heat collectors at their lower end walls, a drying room chimney, a door and 10 racks arranged in 5 storey levels inside. The front drying room, covered by clear glass, is equipped with a front heat exchanger-storage embedded in a biomass furnace provided with flue gas exhaust at its rear while the rear drying room, covered with Glass-Reinforced Concrete (GRC) board, hosts a rear heat exchanger which makes use of the heat of the flue gas. The furnace consists of a floor and walls made of clay-coated concrete, a roof, which is the lower surface of the front heat exchanger base, the flue gas exhaust at the rear end, and a door at the front end. The side walls of the furnace are equipped with eight ventilation holes (4 right and 4 left) as a supplier of fresh air into the furnace while the furnace door only serves the biomass fuel

supply. The solar heat collector consists of a heat-absorbing surface of black-painted corrugated zinc on the upper surface and the lower surface is coated with a glass wool sheet, 5 cm in thickness, used as a heat insulator, installed with an inclination angle of 15° , a roof of clear glass, 5 mm in thickness, and an air inlet at its lower end. The rack is made of an anti-rust wire mesh with 5 mm \times 5 mm square holes with a frame made of galvanised hollow steel pipe, and iron strips, which are used to attach the wire mesh to the frame to strengthen the span of the wire mesh on the frame. Each rack measures 200 cm in length, 87 cm in width and 20 cm in height. The front heat exchanger consists of a vessel made of a 4 mm thickness steel plate equipped with 80 fins (40 on the right and 40 on the left) made of 2 cm thick galvanised hollow steel pipe containing water as the heat storage. The rear heat exchanger consists of a steel plate air hull that accommodates the flue gas from the furnace exhaust and 6 hollow galvanised fresh air channels to absorb the flue gas heat for fresh air heating in-

side and to flow the resulting hot air into the rear drying room. The drying air providing these two heat exchangers in the drying rooms is smoke-free.

On the one hand, the system is operated with solar energy, the front drying room receives the front solar heat collected by the solar collectors and the solar heat from the sunlight passing through the roof, while the rear drying room only receives the heat supply from the rear heat collectors. The received heat is utilised to evaporate the moisture content of the coffee cherries placed on the racks and then the moist air leaving the coffee cherry bed is channelled out from the drying room through the drying chamber chimneys. On the other hand, the system running with the biomass energy, the heat produced by burning the biomass in the furnace is stored by the front heat exchanger and then transferred in the front drying room, and, at the same time, the flue gas heat is transferred into the rear drying room to dry the bed of coffee cherries in both drying rooms. The circulation of the drying air in the heat collector and the drying rooms is performed by natural convection, therefore, the dryer is also free of electricity.

Coffee variety and biomass

The coffee cherries, the Sintaro variety of Robusta, selectively harvested, and only red cherries picked by a smallholder farmer from the Sindang Dataran District-Rejang Regency-Bengkulu Province, Indonesia were used for the experiment. The measured coffee cherry bulk density and the initial moisture contents were $607.66 \text{ kg m}^{-3} (\pm 4.55)$ and $64.26\text{--}65.16\%$ (wet basis), respectively. With this bulk density value, the FETHSBD capacity is up to 4.229 tonnes of coffee cherries.

The biomass used was rubber wood with a moisture content of $8.2\% (\pm 0.5\%)$ (wet basis) and a calorific value of 17.58 MJ kg^{-1} , cut to a length of 60 cm and about a $4 \text{ cm} \times 4 \text{ cm}$ cross section as a fuel supply for the furnace.

Experimental set-up

A Split Plot Experiment Design was employed with two treatments considered, the drying chambers (F_1) (front and rear) as the main plot and the bed thicknesses of the coffee cherries (F_2) (3, 6, 9, 12 cm) as the subplot, and the rack's level (5 levels) as the replication, so 40 samples of coffee cherries were prepared. The coffee cherry samples were filled in a sample box, cube-shaped with 25 cm

sides, made of anti-corrosion wire to be placed inside the drying chambers for the drying process, 20 boxes were arranged in 5 groups of 4 different bed thicknesses to be placed on 5 different rack levels in the front drying chamber and 20 boxes with the same arrangement in the rear drying chamber so that every rack's level was four boxes of different beds (3, 6, 9 and 12 cm) and the rack's levels used were right for the first rack's level, left for the second rack's level, right for the third rack's level, left for forth rack's level, and right for the fifth rack's level. The boxes containing the coffee cherry samples weighed $431.0 \pm 23.0 \text{ g}$ for a bed thickness of 3 cm, $932.2 \pm 60.5 \text{ g}$ for a bed thickness of 6 cm, $1\,327.4 \pm 86.7 \text{ g}$ for a bed thickness of 9 cm and $1\,822.1 \pm 82.7 \text{ g}$ for a bed thickness of 12 cm.

After the sample boxes had been placed in the racks, the rest area of the rack was spread with coffee cherries of about 6 cm bed in thickness. The sample arrangement is presented in Figure 2.

Two series of experiments were performed in July–September 2024, i.e. drying with solar energy and drying with biomass energy so two sets of samples with 80 boxes of coffee cherries were prepared. The solar energy drying was carried out from 9 a.m. to 4 p.m. and continued to the following days until the moisture content of the coffee cherry reached less than 12% wet basis (w.b.). Each day after the drying process was terminated, the sample boxes were taken out from the drying rooms, placed in airtight plastic bags, and stored at room temperature for the next day's experiment.

After the first series of experiments were completed, the biomass energy drying was performed at night from 6 p.m. to 5 a.m. by supplying the furnace with 10 kg rubber wood per hour to produce heat for the drying process employing the same experimental procedure as the first series of experiments.

Variables and measurements

The drying variables observed include the solar radiation intensity (for the solar energy drying), drying air temperature and relative humidity in the drying rooms, ambient temperature and relative humidity, drying air velocity, and sample weight. To conduct measurements, instruments were set up in various places, a ScienPro LT-5000 Model Solarimeter was used near the solar heat collectors, digital thermometers (TMP-10 model) with 0.1% resolution, and a digital hygrometer (HTC-



Figure 2. Sample arrangement – (A) sample boxes, (B) placement of boxes in the rack, (C) racks in the drying room

2 model) were used in the centre of drying rooms and, by a shaded area outside the FETTHSBD, a Hold Peak Model 866B digital manometer was used inside the drying room chimneys whereas the boxes with coffee cherries inside were taken out from the drying rooms to be weighed with a CAMRY Model EK5055 digital balance. The measurements were carried out in a 30-minute interval for the temperature and relative humidity and an hour interval for the drying air velocity and coffee cherry sample weight. The gravimetric oven method was employed to assess the instantaneous coffee cherry sample moisture content on a wet basis based on Equation (1).

$$M_c = \frac{W_w - W_d}{W_w} \times 100 \quad (1)$$

where: M_c , W_w , and W_d – the moisture content (% w.b.), wet weight (g) and dry weight (g), respectively.

The data of the variables were plotted against the drying time.

Coffee bean quality assessment

Number of coffee bean defects (ND) and grade.

The dry coffee cherry samples were processed into coffee beans for a quality assessment according to the Indonesian National Standard for coffee

beans (INS 01-2907-2008) which prescribes a general requirement consisting of no insect contaminant, no spoilage of the seeds, a maximum bean moisture content of 12.5% (w.b.), and a maximum dirt content of the 0.5% mass fraction, and special requirements including the bean size, i.e., big and small seed defects characterised by 17 aspects, and unwanted materials and the quality of coffee beans under investigation are classified in 7 different grades, i.e., Grade 1 (< 11 defects), Grade 2 (12–25 defects), Grade 3 (26–44 defects), Grade 4a (45–60 defects), Grade 4b (61–80 defects), Grade 5 (81–150 defects), and Grade 6 (151–225 defects) found in 300 g of coffee bean seeds. So, the weight of the coffee bean sample prepared for the quality assessment for each treatment was 300 g.

Coffee bean colour. The coffee bean colour was assessed employing a Bioevopek SP-CLR301 colour analyser. On the instrument, the values were read in the form of CIELab L^* , a^* , and b^* . The CIELab colour space shows the colour as three numeric values, L^* for lightness, a^* , and b^* for green-red and blue-yellow components. The values of a^* and b^* can be analysed into the hue angle [$H(^{\circ})$] to analyse the colour degrees as in Equations (2–3). In addition, the a^* and b^* values can also be analysed into the chroma (C), using Equation (4) (Murakonda et al. 2022).

$$H(^{\circ}) = 180 + \tan^{-1} \left(\frac{b^*}{a^*} \right) \quad (\text{for } a^* < 0) \quad (2)$$

$$H(^{\circ}) = \tan^{-1} \left(\frac{b^*}{a^*} \right) \times 57.3 \quad (\text{for } a^* > 0) \quad (3)$$

$$C = \sqrt{(a^*)^2 + (b^*)^2} \quad (4)$$

where: $H(^{\circ})$ – hue angle; a^* , b^* – green-red and blue-yellow components; C – chroma.

Data analysis

Based on the sample moisture content calculated from Equation (1), the measured drying completion time (tc_m) was assessed by the method of interpolation. The moisture content data were also plotted against the drying time and the predicted drying completion time (tc_m) was calculated from the equation of the resulting curve. The tc_m was also plotted against the bed thickness to investigate the potential of the resulting equation to predict the drying time for the wider range. An analysis of variance (ANOVA) was employed for the tc_m , defects value, L^* , H angle, and C with a 5% significant level to look for the effect of the treatments and Duncan's Multiple Range Test (DMRT) was then utilised to analyse for the significant different variables. The SPSS software package (version 27.0) was used to perform the analysis.

RESULT AND DISCUSSION

Profiles of the solar radiation intensity, temperature, relative humidity, and drying air velocity

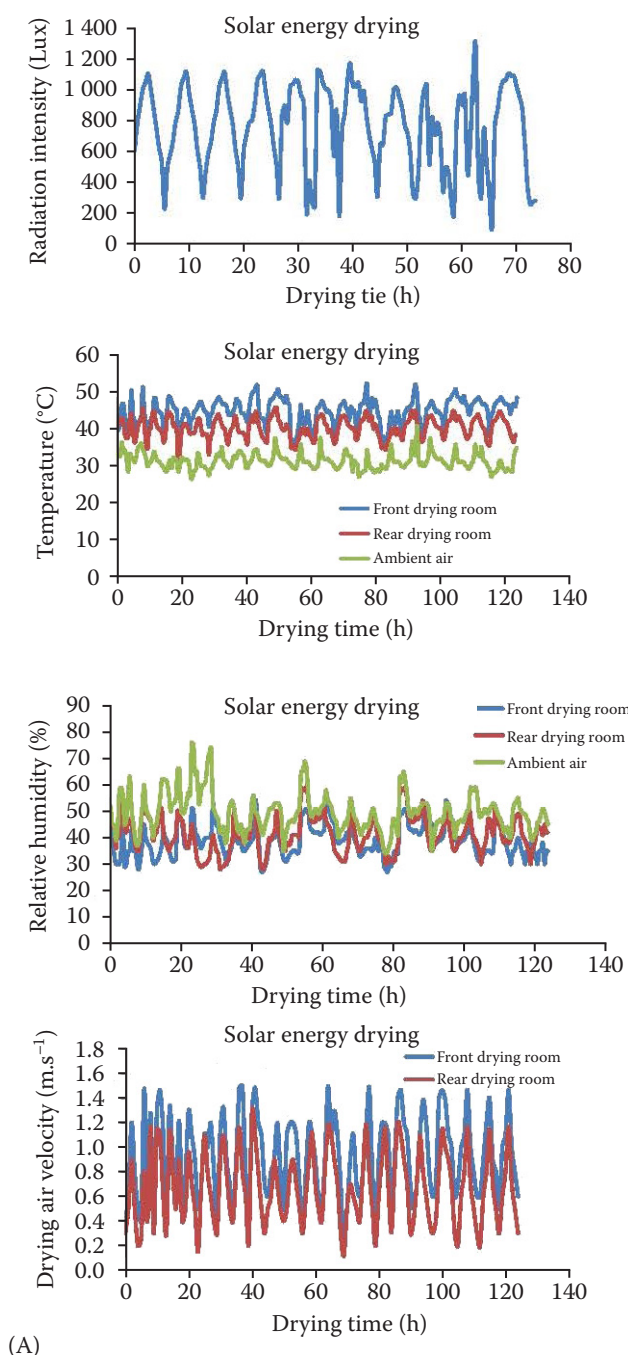
The profiles of the solar radiation intensity, temperature, relative humidity, and drying air velocity are presented in Figure 3. For the solar energy drying, the solar radiation intensity was 755.3 ± 275.7 Lux generating an ambient temperature and relative humidity of 31.1 ± 2.2 °C and $49.6 \pm 7.5\%$, respectively, whereas the drying air temperature, relative humidity, and velocity were 44.6 ± 3.5 °C, $38.8 \pm 6.2\%$, and 0.94 ± 0.33 ms $^{-1}$ for the front drying room and 40.1 ± 2.8 °C, $41.3 \pm 6.8\%$, and 0.67 ± 0.30 ms $^{-1}$ for the rear drying room, respectively. Compared to the reported drying air temperatures and drying air velocities, the temperature of the front drying room was in the middle range of temperatures of the solar dryer (Oria and Palconit 2022;

Mackpayen et al. 2023) and the hybrid solar dryers (Irwansyah et al. 2019; Chan et al. 2020), while the temperature of rear drying room was in the middle range of the solar dryers and in the lower range of the hybrid solar dryers and the drying air velocity of the front drying air was in the upper range of the solar dryers (Hudin et al. 2021; Mackpayen, et al. 2023) and in lower range of the hybrid solar dryers (Yani and Fajrin 2013; Irwansyah et al. 2019) while the drying air velocity of the rear drying room was in the middle range of the solar dryers and in the lower range of the hybrid solar dryers.

The profiles of drying air temperature, relative humidity and velocity of the biomass energy drying were 57.2 ± 3.6 °C, $24.8 \pm 6.0\%$, and 0.91 ± 0.25 ms $^{-1}$ for the front drying room and 45.6 ± 6.0 °C, $33.8 \pm 7.0\%$, and 0.44 ± 0.14 ms $^{-1}$ for the rear drying room, respectively, for the ambient temperature and relative humidity of 26.7 ± 2.0 °C and $74.9 \pm 6.0\%$, respectively. The temperature of the front drying room was in the middle range of the reported temperature range of the mechanical dryers (Nasrin et al. 2021; Konsil et al. 2023) and in the upper range, the reported hybrid dryers (Yani and Fajrin 2013; Irwansyah et al. 2019) and the temperature of the rear drying room was in the middle range of the hybrid solar dryers and in the lower range of the mechanical dryers. The drying air velocity of the front drying room approached that of the solar energy dryers, whereas the drying air of the rear drying room was lower than that of the solar energy dryers.

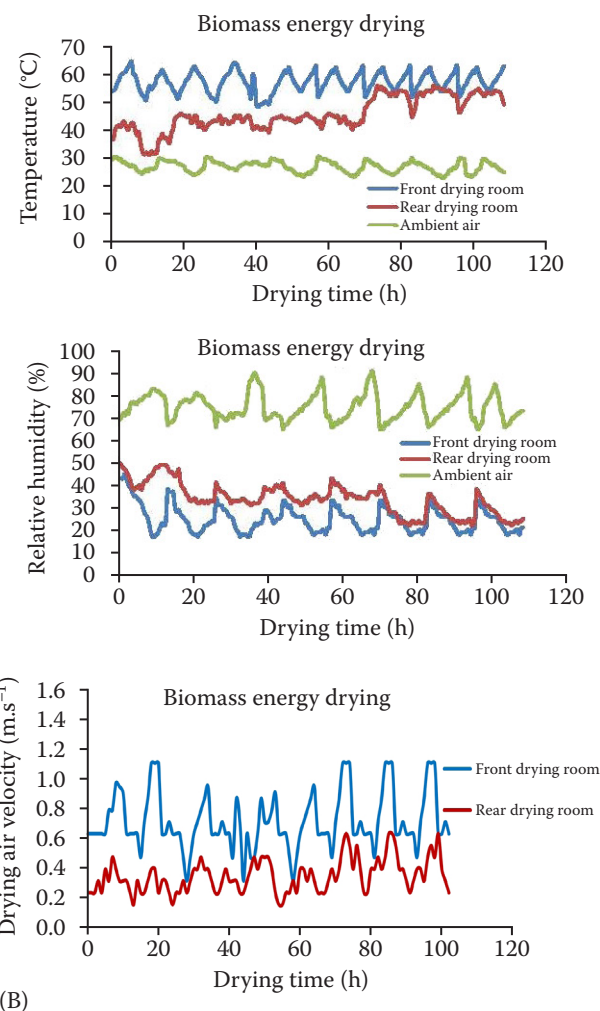
The profiles of tc_m , ND , L^* , $H(^{\circ})$ and C

The tc_m was obtained directly by interpolation of the moisture content data, whereas the tc_p was calculated from the equation of the coffee bean moisture content data plotted against the drying time as presented in Figure 4. For the solar energy drying, the drying curves show that the coffee cherry moisture content decreased linearly against the drying time for both drying rooms with a very high coefficient determination, R^2 approached 0.99, and all the bed thicknesses except the 3 cm bed thickness take up a quadratic trend which had not been reported by other researchers. A linear trend of the curves might exist because there were gradients of the moisture evaporation rate between the outer and inner layers for the thicker bed thicknesses that compensated for each other producing this trend whereas for the 3 cm bed thickness that gradient did not happen producing a different



(A)

Figure 3. Solar radiation intensity, temperature, relative humidity, and drying air velocity – (A) solar energy drying, (B) biomass energy drying



(B)

curve trend between the earlier and later drying process. The drying curves overpredicted the tc_m except for the bed thickness of 3 cm for the front drying room, but gave good prediction results with average errors of 3.96% and 2.12% for the front and rear drying rooms of an overall average error of 3.12%, respectively. This funding is advantageous in practice since linear and quadratic trends are simple, but produce quite accurate results. For the biomass energy drying, the drying curves indicate that the coffee cherry moisture content de-

creased linearly against drying time for the front drying room and decreased quadratically for the rear drying room with very high R^2 values. The drying curves predicted a tc_m with average errors of 3.66% and 1.98% for front and rear drying rooms, respectively, or an overall average error of 2.36% which were lower than those of the solar energy drying, suggesting a better prediction result. The tc_m together with its standard of deviation and tc_p together with the prediction error are presented in Table 1.

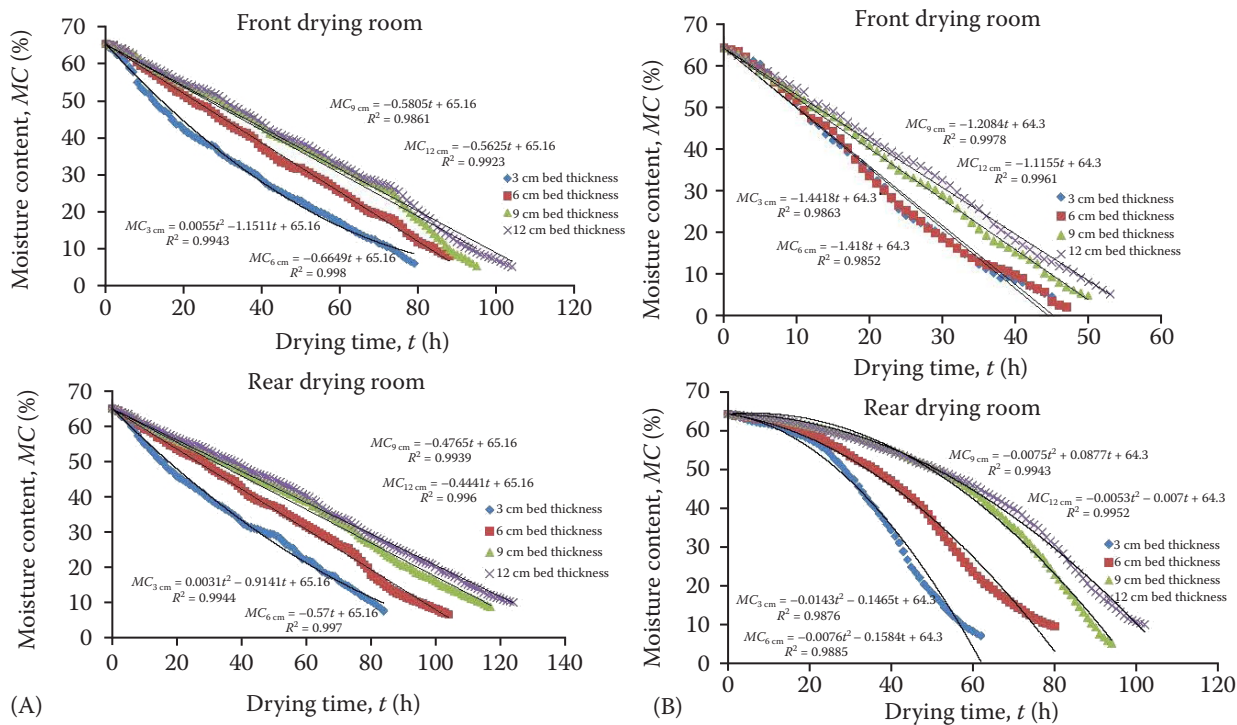


Figure 4. Coffee bean moisture content plotted against the drying time for the solar energy drying – (A) solar energy drying, (B) biomass energy drying

Table 1. The values of the drying air temperature, drying completion times (observed and predicted), number of defects, colour lightness, hue and chroma

Drying room	Bed thickness (cm)	Drying air temperature (°C)	tc_m (h)	tc_p (h)	Prediction error (%)	ND	L^*	$H(^{\circ})$	C
FDR	3	44.6 ± 3.5	70.9 ± 10.6	68.8 ± 11.7	2.9	7.2 ± 0.11	42.4 ± 4.41	179.1 ± 0.66	21.6 ± 20.0
	6		76.7 ± 12.2	80.0 ± 17.0	-4.2	6.6 ± 0.13	48.8 ± 4.58	179.2 ± 0.59	20.0 ± 19.0
	9		83.5 ± 11.0	91.6 ± 23.7	-9.7	6.3 ± 0.09	44.4 ± 4.52	179.0 ± 0.71	18.0 ± 16.6
SER	12	40.1 ± 2.8	90.2 ± 11.5	94.5 ± 26.5	-4.8	5.8 ± 0.15	46.8 ± 3.33	179.1 ± 0.60	17.1 ± 15.6
	3		77.2 ± 5.2	80.1 ± 4.6	3.7	5.5 ± 0.08	44.2 ± 4.84	179.1 ± 0.60	20.0 ± 2.54
	6		92.8 ± 10.8	93.3 ± 7.7	0.5	5.1 ± 0.11	48.3 ± 5.47	179.0 ± 0.60	19.0 ± 1.35
RDR	9	40.1 ± 2.8	109.3 ± 5.6	111.6 ± 7.5	2.0	4.4 ± 0.13	49.2 ± 4.69	179.0 ± 0.63	16.6 ± 2.79
	12		116.5 ± 5.5	119.7 ± 11.6	2.8	4.2 ± 0.07	48.1 ± 6.91	179.1 ± 0.65	15.6 ± 1.54
	3		34.1 ± 9.2	36.3 ± 10.6	6.3	4.5 ± 0.07	34.6 ± 4.87	179.1 ± 0.73	179.1 ± 0.73
FDR	6	57.2 ± 3.6	37.1 ± 8.3	36.9 ± 8.1	-0.5	5.1 ± 0.13	35.6 ± 5.73	179.2 ± 0.60	179.2 ± 0.60
	9		41.5 ± 8.0	43.3 ± 11.4	4.4	5.3 ± 0.11	39.9 ± 4.24	179.0 ± 0.74	179.0 ± 0.74
	12		44.9 ± 7.4	46.9 ± 8.1	4.4	7.1 ± 0.13	37.7 ± 2.45	179.1 ± 0.67	179.1 ± 0.67
BED	3	45.6 ± 6.0	56.3 ± 3.9	55.6 ± 7.0	-1.3	4.6 ± 0.10	40.4 ± 8.27	179.7 ± 1.24	179.7 ± 1.24
	6		73.6 ± 2.9	73.2 ± 7.3	-0.6	5.5 ± 0.14	41.2 ± 6.83	179.0 ± 0.70	179.0 ± 0.70
	9		86.3 ± 5.0	89.6 ± 33.0	3.8	7.8 ± 0.05	39.7 ± 5.34	179.6 ± 1.20	179.6 ± 1.20
	12		96.4 ± 2.6	98.7 ± 23.2	2.3	8.5 ± 0.38	43.9 ± 6.88	179.1 ± 0.66	179.1 ± 0.66

INS – Indonesian National Standard; SER – solar energy drying; BED – biomass energy drying; FDR – front drying room; RDR – rear drying room; ND – number of defects (determined from 12 INS parameters relevant to the drying process); L^* – clarity, in which $L = 0$ is black, and $L^* = 100$ is colourless; $H(^{\circ})$ – the tonality was the characteristics of the colour, i.e. red, yellow, green, and blue; C – chroma = the level of colour related to a lower or higher intensity of the colour

Number of coffee bean defects (ND). The profile of the number of coffee bean defects is presented in Table 1 and all the treatments produced $NDs < 11$ qualified for Grade 1, for the solar energy drying, the average values were 6.48 and 4.82 for the front and rear drying room, respectively, or an overall of 5.64, while for the biomass energy drying, the average values were 5.51 and 6.98 for the front and rear drying room, respectively, or an overall of 6.06. These quality grades were comparable to the quality grades of the coffee beans of the same variety processed with the fully washed method reported by Budiyanto et al. (2021). Since the numbers were still far less than 11, it suggested that the bed thickness may be increased for further research to maximise the drying performance.

Coffee bean colour. The profile of the assessed coffee bean is presented in Table 1 and Figure 5. The averages of L^* , H^0 , and C were 45.6, 179.1, and 19.2 for the front drying room and 48.0, 179.1, and 17.4 for the rear drying room or 46.5, 179.1, and 18.5 overall, respectively. The general characteristic

of this colour was yellowish green. The L^* value confirmed the L^* value reported by Harijono et al. (2024), i.e. 46.73 which was obtained from coffee beans dried with a dome solar dryer and lower than that assessed from commercial lots of the Robusta variety in Brazil by Bicho et al. (2014) which was 57.3. Bicho et al. (2014) also reported an H^0 of 79.4 and a C of 16.52 which were very much lower and higher than those found in this study.

ANOVA and DMRT analyses

ANOVA and DMRT for solar energy drying. The results of the ANOVA and DMRT for solar energy drying are summarised in Table 2. The drying room, bed thickness, and the interaction of the drying room-bed thickness significantly affected the tc_m and ND and the bed thickness only significantly affected C . The result of the DMRT demonstrated the tc_m was significantly different among the other values, whereas an ND of 3 cm was significantly different from the other bed thicknesses and there was no significant difference among the



Figure 5. Coffee bean colour – (A) solar energy drying, (B) biomass energy drying
F – front drying room; R – rear drying room, 3 cm to 12 cm bed thickness

Table 2. Results of ANOVA and DMRT analyses for solar energy drying

ANOVA variable	Source of variation			DMRT variable			
	Drying room (F_1)	Bed thickness(F_2)	$F_1 \times F_2$	Bed thickness (cm)	tc_m	ND	C
tc_m	*	*	*	3	74.4 ^a	6.4 ^a	20.8 ^a
ND	*	*	*	6	84.7 ^b	5.8 ^b	19.5 ^a
L^*	ns	ns	ns	9	96.4 ^c	5.4 ^b	17.3 ^b
$H(^{\circ})$	ns	ns	ns	12	103.3 ^d	5.0 ^b	16.3 ^b
C	ns	*	ns	—	—	—	—

Significantly different ($P < 0.05$); ^{a–d}numbers with the same letter subscript = not significantly different, numbers with the different letter subscript = significantly different; ANOVA – analysis of variance; DMRT – Duncan's Multiple Range Test; tc_m – completion time; ND – number of defects; L^ – clarity, in which $L = 0$ is black, and $L^* = 100$ is colourless; $H(^{\circ})$ – the tonality was the characteristics of the colour, i.e. red, yellow, green, and blue; C – chroma = the level of colour related to a lower or higher intensity of the colour; ns – not significantly different ($P > 0.05$)

bed thicknesses of 6, 9, and 12 cm, and there were no significant between the Cs of the 3 and 6-bed thicknesses and there were significant differences in the Cs of the 3 and 6 cm bed thickness from those of the 9 and 12 cm bed thicknesses, and there was no significant difference between the Cs of the 9 and 12 cm bed thicknesses. Since the ND found in this study was still much lower than 11, it was advantageous to plot these three parameters with the bed thickness to look for the possibility of setting up a drying process for the higher bed thickness to maximise the performance of the dryer and the results are presented in Figure 6. The curves of the parameters versus the bed thickness exhibited very high R^2 (0.99) suggesting that the bed thickness was very reliable in predicting the three parameters and, since the trend of the ND curve was negative, it would be possible to employ a bed thickness higher than 12 cm until the full capacity

of the dryer of about 4.229 tonnes of coffee cherries is reached.

The curve of the tc_m versus the bed thickness versus can be employed to benchmark the performance of this dryer to the dryers of a similar type. The result of this solar energy drying can be compared to the performances of the solar dryers investigated by Harijono et al. (2024) and Widjotomo (2014).

Employing a dome solar dryer, Harijono et al. (2024) dried a 5 cm bed thickness from a 50.67% moisture content to 12.7% in 21 days and Widjotomo (2014) utilising a big scale solar dryer dried a 60 kg m^{-2} bed thickness from 9.87 cm calculated using a bulk density of 607.66 kg m^{-3} from 64.16% to 12.28% in 120 hours. From the equation of the above curve, $tc_m = 3.2824T + 65.094$, the drying processes of 5 cm and 9.87 cm bed thicknesses could be completed in 81.506 h and 97.491 h, respectively, demonstrating that the FETTHSBD

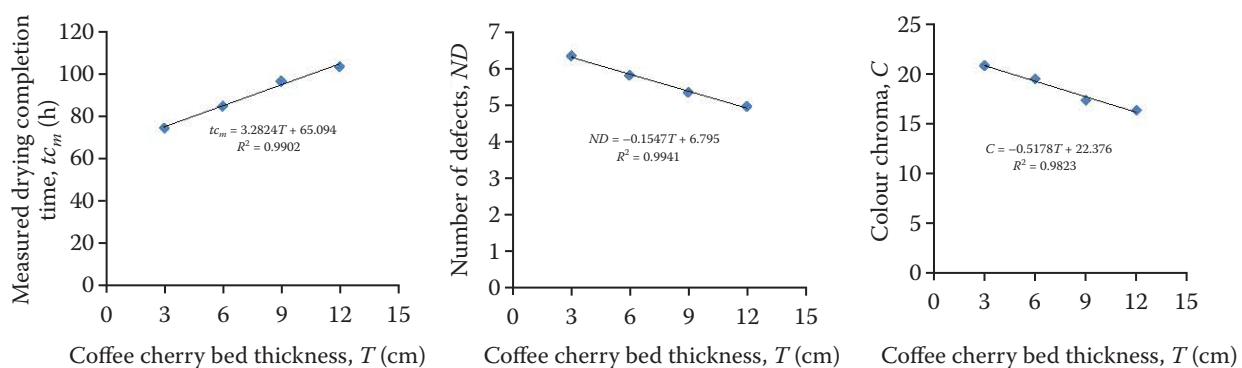


Figure 6. The measured drying completion time, number of defects, and colour chroma plotted against the coffee cherry bed thickness for solar energy drying

tc_m – completion time; ND – number of defects (determined from 12 INS parameters relevant to the drying process); C – chroma = the level of colour related to a lower or higher intensity of the colour; INS = Indonesian National Standard

performed better than Harijono's dryer and Widjotomo's dryer.

ANOVA and DMRT analyses for the biomass energy drying. The results of the ANOVA and DMRT are summarised in Table 3 indicating that the results of the ANOVA were the same as that of the solar energy drying. The results of the DMRT for the tc_m and ND indicated that the t12% and ND were different among the bed thicknesses, whereas there were no significant between the C s of the 3 cm and 6 cm bed thicknesses and there were significant differences between the C s of the 3 cm and 6 cm bed thickness from those of the 9 cm and 12 cm bed thicknesses, and there was no significant difference between the C s of the 9 and 12 cm bed thicknesses. The tc_m , ND , and C were plotted against the bed thicknesses as shown in Figure 7.

In terms of the tc_m , the biomass energy drying might be compared to the solar-biomass hybrid

dryer proposed by Chan et al. (2020). As described before, the FETTHSBD was constructed of two drying rooms containing 20 racks each, 2 solar heat collectors, and a furnace with a total structure area of 30 m² whereas Chan's dryer consisted of a drying room functioning as the solar heat collector and contained 4 shelves and a furnace with a total building area of 25.44 m². When operated with solar heat and followed by the combustion heat of 5 kg of firewood per hour for 11.33 h per day, Chen's dryer generated 43.6 °C on average and reduced 800 kg of coffee cherries from 65% to 12% in 79.3 hours. Operated with 10 kg firewood per hour, the FETTHSBD generated 57.2 °C and 45.6 °C for the front and rear drying rooms, respectively, or 51.4 °C on average and it was reasonable for comparison since it was more than four times larger than that of Chan's dryer. With a 607.66 kg/m³ coffee cherry bulk density, 800 kg coffee cherries were equivalent

Table 3. Results of the ANOVA and DMRT analyses for the biomass energy drying

ANOVA variable	Source of variation			DMRT variable			
	Drying room (F_1)	Bed thickness (F_2)	$F_1 \times F_2$	Bed thickness (cm)	tc_m	ND	C
tc_m	*	*	*	3	45.2 ^a	4.6 ^a	23.6 ^a
ND	*	*	*	6	55.4 ^b	5.3 ^b	21.8 ^a
L^*	ns	ns	ns	9	63.9 ^c	6.6 ^c	19.9 ^b
$H(^{\circ})$	ns	ns	ns	12	70.7 ^d	7.8 ^d	18.2 ^b
C	ns	*	ns	—	—	—	—

Significantly different ($P < 0.05$); ^{a-d}numbers with the same letter subscript – not significantly different, number with the different letter subscript – significantly different; ANOVA – analysis of variance; DMRT – Duncan's Multiple Range Test; tc_m – completion time; ND – number of defects; L^ – clarity, in which $L = 0$ is black, and $L^* = 100$ is colourless; $H(^{\circ})$ – the tonality was the characteristics of the colour, i.e. red, yellow, green, and blue; C – chroma = the level of colour related to a lower or higher intensity of the colour; ns – not significantly different ($P > 0.05$)

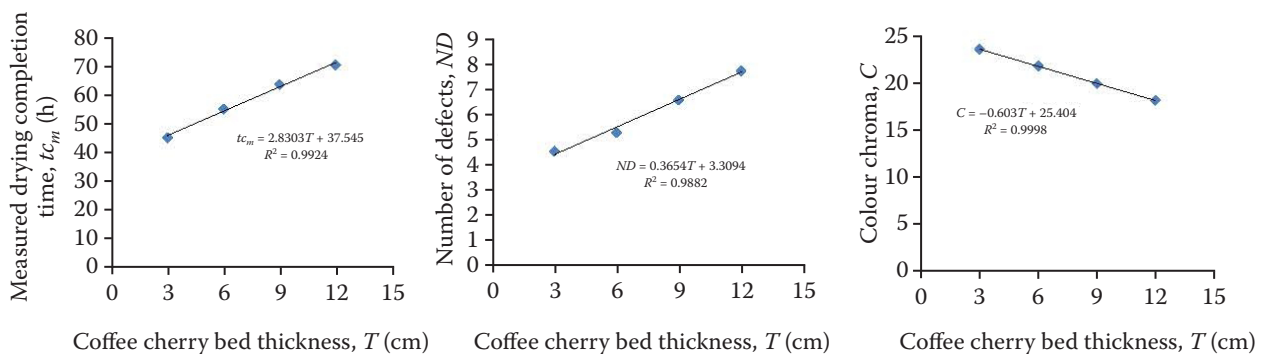


Figure 7. The measured drying completion time, number of defects, and colour chroma plotted against the coffee cherry bed thickness for the biomass energy drying

tc_m – completion time; ND – number of defects (determined from 12 INS parameters relevant to the drying process); C – chroma = the level of colour related to a lower or higher intensity of the colour; INS – Indonesian National Standard

to a 1.89 cm bed thickness, and using the equation of the curve in Figure 10, i.e., $tc_m = 2.803 T + 37.545$, the drying processes of 1.89 cm bed thicknesses should be completed in 42.84 h suggesting that the FETTHSBD performed better than Chen's dryer.

CONCLUSION

A free electricity tandem-twin-hybrid solar-biomass dryer was studied operating with solar and biomass energies separately to dry Robusta coffee cherries with the respect to the drying rooms, the front and rear and cherry bed thicknesses of 3, 6, 9, and 12 cm were employed using a split plot design experiment. The result of the ANOVA indicated that the drying rooms, bed thickness, and the interaction of the drying room-bed thickness significantly affected the drying completion time, tc , and number of defects, ND , and only the bed thickness significantly affected the chroma, C , for both the solar energy drying and the biomass energy drying. On one hand, the result of the DMRT for the solar energy drying demonstrated that the tc was significantly different among the other values, whereas an ND of 3 cm was significantly different from the other bed thicknesses and there was no significant difference among the bed thicknesses of 6, 9 and 12 cm, and there were no significant between the Cs of the 3 and 6 cm bed thicknesses and there were significant differences in the Cs of the 3 cm and 6 cm bed thickness from those of the 9 cm and 12 cm bed thicknesses, and there was no significant difference between the Cs of the 9 and 12 cm bed thicknesses. The results of the DMRT for tc_m and ND indicated that the tc and ND were different among the bed thicknesses, whereas there were no significant differences between the Cs of the 3 cm and 6 cm bed thicknesses and there was a significant difference between the Cs of the 3 cm and 6 cm bed thickness from those of the 9 cm and 12 cm bed thicknesses, and there was no significant difference between the Cs of the 9 cm and 12 cm bed thicknesses. The biomass energy drying with a 10 kg rubber wood supply per hour sped up the completion of the drying process from 89.64 h to 58.78 h and maintained the quality of the resulting coffee beans in Grade 1.

Acknowledgment: We thank to Agricultural Technology Laboratory, University of Bengkulu for instrumentation support.

REFERENCES

Al-Kindi H., Purwanto Y.A., Wulandani D. (2015): Analisis CFD aliran udara panas pada pengering tipe rak dengan sumber energi gas buang [Distribution analysis of hot air flow in rack type dryer with energy source from exhaust gas using Computational Fluid Dynamics (CFD)]. *Jurnal Keteknikan Pertanian*, 3: 9–16 (in Indonesian).

Bicho N., Ramalho J.C., Leitão A., Lidon F.C. (2014): Application of colour parameters for assessing the quality of Arabica and Robusta green coffee. *Emirates Journal of Food and Agriculture*, 26: 9–17.

Budiyanto, Izahar T., Ukker D. (2021): Karakteristik fisik kualitas biji kopi dan kualitas kopi bubuk Sintaro 2 dan Sintaro 3 dengan berbagai tingkat sangrai (Physical characteristics of coffee beans and quality of ground coffee Sintaro 2 and Sintaro 3 with various roast levels). *Jurnal Agroindustri*, 11: 54–71 (in Indonesian).

Chan Y., Sugiyanto D., Uyun A.S. (2020): Analisis pengeringan kopi menggunakan oven pengering hybrid (solar thermal dan biomassa) di Desa Gununghalu [Coffee drying analysis using a hybrid drying oven (solar thermal and biomass) in Gununghalu Village]. *Jurnal Kajian Teknik Mesin*, 5: 4–8 (in Indonesian).

Dzaky M.I., Kosasih E.A., Hakim I.I., Zikri A. (2023): Investigation of thin-layer drying of coffee beans using a double-condenser compression refrigeration system: Effects of air mass flux, specific humidity and drying temperature. *Journal of Advanced Research in Fluid Mechanics and Thermal Sciences*, 106: 90–103.

Fatharani A., Yuwana Y., Yusuf D., Hidayat L. (2023): Drying characteristics of robusta coffee beans using YSDUNIB18 hybrid dryer based on thin-layer drying kinetics fitting model. *International Journal of Agricultural Technology*, 19: 37–52.

Firdissa E., Mohammed A., Berecha G., Garedew W. (2022): Coffee drying and processing method influence quality of arabica coffee varieties (*Coffea arabica* L.) at gomma I and limmu kossa, southwest Ethiopia. *Journal of Food Quality*, 3: 1–8.

Gachen A., Hirpersa Z., Woyessa L.N. (2020): Design and construction of indirect solar coffee dryer. *International Journal of Innovative Technology and Exploring Engineering (IJITEE)*, 9: 2943–2956.

Gunawan Y., Margono K.T., Rizky R., Putra N., Al Fatih R., Hakim I.I., Setiadanu G.T., Suntoro D., Kasbi S., Nafis S. (2021): Enhancing the performance of conventional coffee beans drying with low-temperature geothermal energy by applying HPHE: An experimental study. *De Gruyter*, 6: 807–818.

Harijono, Wicaksono M.F., Wulan S.N., Ali Y.S. (2024): Changes in physico-chemical characteristics of robusta

coffee (*Coffea canephora*) during natural process using simple solar dryer. BIO Web of Conferences, 90: 01003.

Hidayat R., Ubaidillah F., Siswanto H. (2018): Optimasi proses pengeringan kopi di pabrik kopi PTPN XII Guitir dengan menggunakan mason dryer (Optimization of the coffee drying process at the PTPN XII Guitir Coffee Factory using a Mason dryer). Jurnal Ilmiah Matematika dan Pendidikan Matematika (JMP), 10: 17–30 (in Indonesian).

Hudin T.J., Koehuan V.A., Nurhayati (2021): Perancangan rumah pengering biji kopi menggunakan plastik ultra violet (UV solar dryer) dengan mekanisme konveksi alamiah [Design of coffee bean drying house using ultraviolet plastic (UV solar dryer) with natural convection mechanism]. Lontar: Jurnal Teknik Mesin Undana, 8: 25–39 (in Indonesian).

Irwansyah I., Nelwan L.O., Wulandari D. (2019): Desain dan uji kinerja alat pengering hybrid dengan efek cerobong tipe tumpukan untuk pengeringan biji kopi Arabika (Design and performance test of hybrid dryer with chimney effect pile type for drying Arabica coffee beans.). Jurnal Keteknikan Pertanian, 7: 163–170 (in Indonesian).

Konsil K.K., Sazali N., Kadrigama K., Harun W.S.W., Zainol N. (2023): Analysis on the performance of designed fluidized bed dryer for drying coffee beans. Journal of Advanced Research in Applied Sciences and Engineering Technology, 31: 99–109.

Largo-Avila E., Suarez-Rodriguez C.H., Montero J.L., Strong M., Osorio-Aries J. (2023): The influence of hot-air mechanical drying on the sensory quality of specialty Colombian coffee. AIMS Agriculture and Food, 8: 789–803.

Mackpayen A.O., Akata A.M.E.A., Barandja V.D.D.B., Napo K. (2023): Experimental study of a modified icaro solar dryer: The case of coffee drying. Journal of Power and Energy Engineering, 11: 36–48.

Murakonda S., Patel G., Dwivedi M. (2022). Characterization of engineering properties and modeling mass and fruit fraction of wood apple (*Limonia acidissima*) fruit for post-harvest processing. Journal of the Saudi Society of Agricultural Sciences, 21: 267–277.

Murdianto D., Santoso D. (2019): Pemodelan mesin pengering biji-bijian tipe batch menggunakan hybrid petri net (Modeling of batch type seed dryer machine using a petri net hybrid). Perbal: Jurnal Pertanian Berkelanjutan, 7: 115–120 (in Indonesian).

Nasrin A.B.M.S., Tan A.S.T., Huey C.N., Abdullah A., Ismail W.A.A.Z.W., Januar J. (2021): Drying characteristics and nutritive analysis of coffee beans under different drying methods. Transaction on Science and Technology, 8: 439–444.

Oria C.L. Palconit E.V. (2022): Performance investigation of an inflatable solar dryer with steel-can solar air heater for drying coffee and corn. Engineering, Technology & Applied Science Research, 12: 8707–8711.

Peñuela-Martínez A.E., Hower-Garcia I.P., Guerrero A., Agudelo-Laverde L.M., Betancourt-Rodriguez H., Martinez-Giraldo J. (2023): Physical, sensorial, and physico-chemical characteristics of Arabica coffee dried under two solar brightness conditions. Processes, 11: 2–17.

Phitakwinai S., Thepa S., Nilnont W. (2019): Thin-layer drying of parchment Arabica coffee by controlling temperature and relative humidity. Food Science & Nutrition, 7: 2921–2931.

Prasetya R.A., Irfai M.A., Samudra A. (2020): Rancang bangun alat pengering biji kopi menggunakan pemanas kompor gas LPG dengan model roll (Design and construction of coffee bean dryer using heater LPG stove with roll model). Reaktom: Rekayasa Keteknikan dan Optimasi, 5: 14–21 (in Indonesian).

Putra I. E., Hadi P. (2013): Analisa efisiensi alat pengering tenaga surya tipe terowong berbantuan kipas angin pada proses pengeringan biji kopi (Efficiency analysis of a fan-assisted tunnel type solar dryer in the coffee bean dryng process). Jurnal Teknik Mesin, 3: 22–25 (in Indonesian).

Siagian P., Napitupulu F.H., Ambarita H., Sihombing H.C., Siagian H. (2024): Comparative analysis of coffee drying on quality with variations in dryers made solar collectors. AIP Conference Proceedings, 3048: 020042.

Soeswanto B., Wahyuni N.L.E., Prihandini G., Pratama Y., Firmansyah T.A., Widayabudiningsih D. (2023): Effect of process variables and zeolite adsorbent in coffee bean drying. Current Journal International Journal Applied Technology Research, 4: 29–40.

Suherman S., Widuri H., Patricia S., Susanto E.E., Sutrisna R.J. (2020): Energy analysis of a hybrid solar dryer for drying coffee beans. International Journal of Renewable Energy Development, 9: 131–139.

Sutrisno, Ariwibowo D., Yulianto M.E., Sitawati R. (2020): Characteristic of vertical mixed flow dryer in coffee bean drying process. IOP Conf. Series: Materials Science and Engineering, 771: 012070.

Widyotomo S. (2014): Kinerja bangunan tembus cahaya skala besar untuk proses pengeringan kopi (Performance of a large scale green house for coffee drying process). Pelita Perkebunan, 30: 240–257 (in Indonesian).

Yani E., Fajrin S. (2013): Karakteristik pengeringan biji kopi berdasarkan variasi kecepatan aliran udara pada solar dryer (Drying characteristics based on the variation of drying air velocity of solar dryer solar dryer). TeknikA, 20: 17–22 (in Indonesian).

<https://doi.org/10.17221/98/2024-RAE>

Yuwana Y., Silvia E., Sidebang B. (2021): Coffee cherries drying trials utilizing the hybrid solar dryer. *Advances in Biological Sciences Research. Proceedings of the International Seminar on Promoting Local Resources for Sustainable Agriculture and Development (ISPLRSAD 2020)*, 13: 497–503.

Yuwana Y., Sidebang B. (2023): Performance testing of the tandem hybrid solar-biomass dryer for coffee cherry drying. *International Journal of Agricultural Technology*, 19: 1969–1982.

Received: December 16, 2024

Accepted: June 18, 2025

Published online: September 26, 2025